



Cite this: *Green Chem.*, 2026, **28**, 3232

Palladium-catalyzed asymmetric sequential hydroalkylation and hydroamination of 1,3-enynes with 3-hydroxyindoles

Qiuyu Li,^{†a} Ruixue Wu,^{†a} Tianbao Wu,^{†b} Renkang Wei,^a Zhijiao Li,^a Shang Gao,^{id a} Minyan Wang,^{*b} Hequan Yao^{id *a} and Aijun Lin^{id *a}

Transition-metal catalyzed asymmetric hydrofunctionalization of unsaturated hydrocarbons has emerged as an efficient method to access diverse chiral value-added compounds. In contrast, asymmetric sequential hydrofunctionalization cyclization, which could incorporate two functional groups across carbon-carbon multiple bonds to construct chiral complex cyclic compounds, has only been sporadically explored. Herein, we report a palladium-catalyzed asymmetric sequential hydroalkylation and hydroamination of readily available 1,3-enynes with 3-hydroxyindoles. This redox-neutral process provides an efficient route for constructing a broad spectrum of enantioenriched pyrido[1,2-*a*]indoles and derivatives with high atom- and step-economy. Preliminary mechanistic investigations reveal that this transformation proceeds *via* an intermolecular enyne hydroalkylation pathway to produce an allene intermediate. Subsequent intramolecular hydroamination of the allene intermediate occurs *via* an axial-to-center chirality transfer process. Density functional theory (DFT) studies were conducted to probe the origin of enantioselectivities.

Received 18th October 2025,
Accepted 10th January 2026

DOI: 10.1039/d5gc05558j

rsc.li/greenchem

Green foundation

1. This palladium-catalyzed asymmetric sequential hydroalkylation/hydroamination of 1,3-enynes achieves 100% atom economy under redox-neutral conditions, minimizing waste by incorporating all atoms of the starting materials into the final products.
2. This asymmetric sequential hydrofunctionalization cyclization can install two distinct functional groups across the unsaturated hydrocarbons in one pot with excellent step economy.
3. The enantioenriched pyrido[1,2-*a*]indoles and derivatives are constructed with high efficiency with excellent chemo-, enantio-, and diastereo-selectivity (up to >20 : 1 rr, >20 : 1 dr, 97% ee). The gram-scale capability further underscores the practical efficiency and sustainability of this methodology.

Introduction

With increasing concerns about environmental sustainability, preparing value-added molecules such as bioactive compounds and pharmaceuticals, from readily available materials in a redox-neutral, atom- and step-economical manner has been a hot topic for the synthetic and medicinal communities.¹ One of the versatile strategies to achieve this goal is to develop transition-metal catalyzed hydrofunctionalization of unsaturated hydrocarbons, which provides synthetically valuable products with 100% atom utilization.² Over the past decades, great efforts

have been made in the catalytic asymmetric hydrofunctionalization of alkenes,³ alkynes,⁴ allenes,⁵ and dienes,⁶ facilitating the construction of alkyl and allyl compounds. Recently, the asymmetric hydrofunctionalization of conjugated enynes has garnered attention and warrants further study. In this context, the groups of Buchwald, Hoveyda, Malcolmson, Engle, He and Luo have independently gained elegant achievements for the synthesis of optically pure allene and propargyl compounds (Scheme 1a).⁷ However, these advancements have predominantly concentrated on the introduction of a single functional motif onto unsaturated hydrocarbons.

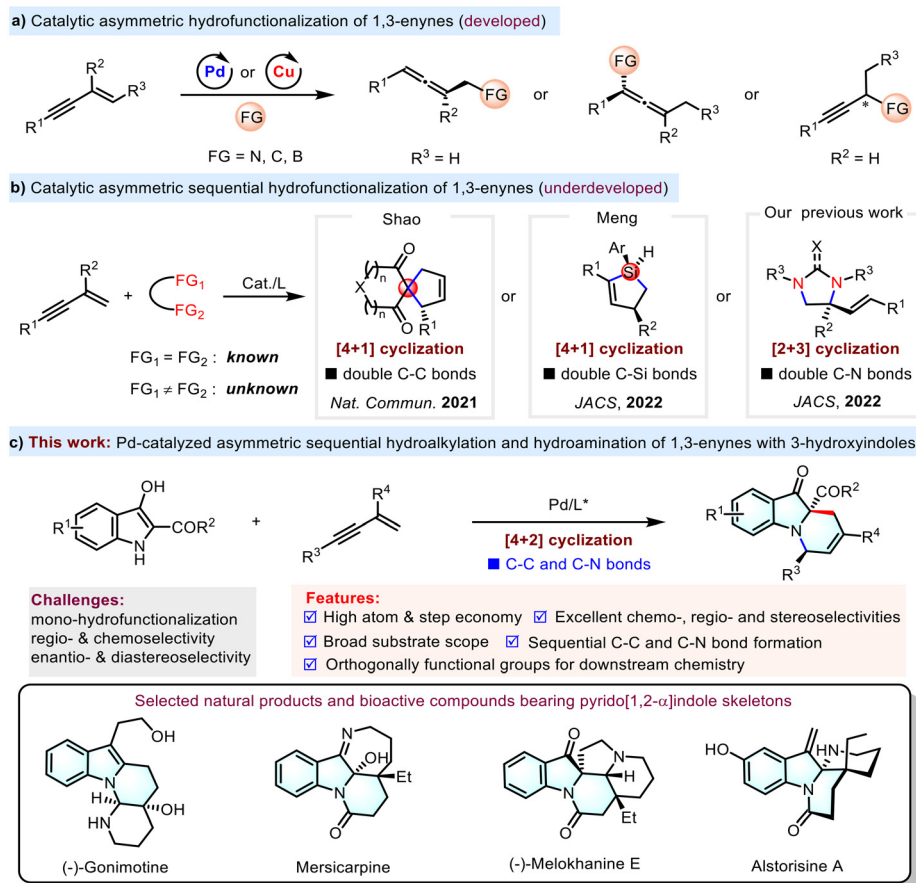
Sequential reactions, which could incorporate several transformations into a single sequence, represent a powerful strategy to rapidly install two or more functional groups to construct complex molecules in a step-economical fashion.⁸ In this regard, asymmetric sequential hydrofunctionalization of conjugated enynes provides a unique approach to assembling structurally diverse chiral cyclic compounds. Nevertheless,

^aState Key Laboratory of Natural Medicines (SKLNM) and Department of Medicinal Chemistry, School of Pharmacy, China Pharmaceutical University, Nanjing, 210009, P. R. China. E-mail: hyao@cpu.edu.cn, ajlin@cpu.edu.cn

^bState Key Laboratory of Coordination Chemistry, School of Chemistry and Chemical Engineering, Nanjing University, Nanjing 210093, China

[†]These authors contributed equally to this work.





Scheme 1 Catalytic asymmetric hydrofunctionalization of 1,3-enynes.

only a few asymmetric variants have been disclosed to date. In 2021, the Shao group developed a palladium-catalyzed sequential hydroalkylation of 1,3-enynes (double C–C bond formation) to produce a panel of chiral spiro compounds in good yields.⁹ In 2022, Meng and coworkers described a Co-catalyzed sequential hydrosilylation of 1,3-enynes (double C–Si bond formation) to generate enantioenriched cyclic alkenylsilane scaffolds with a high level of enantioinduction.¹⁰ In addition, our group reported a Pd-catalyzed sequential hydroamination of 1,3-enynes and ureas *via* the formation of double C–N bonds, yielding valuable chiral imidazolindione architectures (Scheme 1b).¹¹ Despite this progress, the installation of two distinct functional groups *via* the asymmetric sequential hydrofunctionalization of enynes has thus far proven elusive.¹²

As an extension of our interest in the catalytic hydrofunctionalization of unsaturated hydrocarbons,^{11,13} we seek to integrate hydroalkylation and hydroamination with 3-hydroxyindoles as nucleophiles, fulfilling the more challenging asymmetric sequential hydrofunctionalization of 1,3-enynes (Scheme 1c). However, the realization of this procedure in one pot presents several sticky issues. (1) The reaction might terminate prematurely at the first stage, leading to the formation of allene or diene products. (2) Both 3-hydroxyindoles and 1,3-enynes contain multiple reaction sites, complicating precise

control over chemo- and regioselectivity. (3) Achieving control over the enantioselectivity and diastereoselectivity of the products poses an additional challenge.

Herein, we report an unprecedented palladium-catalyzed asymmetric sequential hydroalkylation and hydroamination

Table 1 Optimization of the racemic reaction conditions^{a,b,c}

Entry	[Pd] source	Solvent	Yield (%)	dr
1	Pd(OAc) ₂	DCM	30	10 : 1
2	Pd(OAc) ₂	1,4-Dioxane	54	15 : 1
3	Pd(OAc) ₂	Toluene	59	13 : 1
4	Pd(acac) ₂	Toluene	65	>20 : 1
5	[Pd(π -allyl)Cl] ₂	Toluene	75	>20 : 1

^a Standard conditions: **1a** (0.2 mmol), **2a** (0.4 mmol), [Pd] (10 mol%), Xantphos (20 mol%), PhCOOH (20 mol%), solvent (1.0 mL), at 80 °C under an Ar atmosphere for 48 h. ^b Isolated yield. ^c The dr values were determined by crude ¹H NMR.



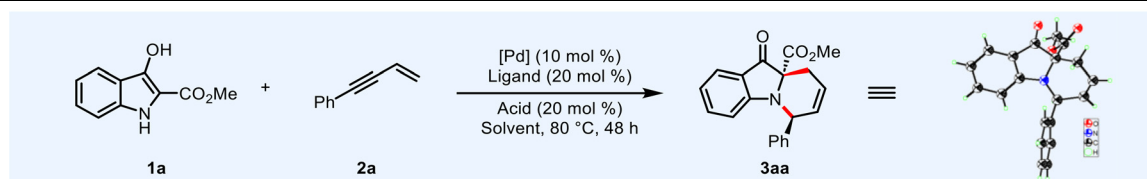
reaction between 3-hydroxyindoles and 1,3-enynes to yield optically pure pyrido[1,2-*a*]indoles and derivatives in good efficiency. This process demonstrates excellent regio-, chemo-, and stereoselectivities, along with commendable atom- and step-economy. These scaffolds constitute a structurally fascinating part of indole alkaloids, which are prevalent in a variety of natural products and bioactive compounds.¹⁴ Preliminary mechanistic studies disclose that this consecutive reaction proceeds through an intermolecular enyne hydroalkylation pathway to yield an allene intermediate. The subsequent intramolecular hydroamination of the allene intermediate involves an axial-to-center chirality transfer process.

Results and discussion

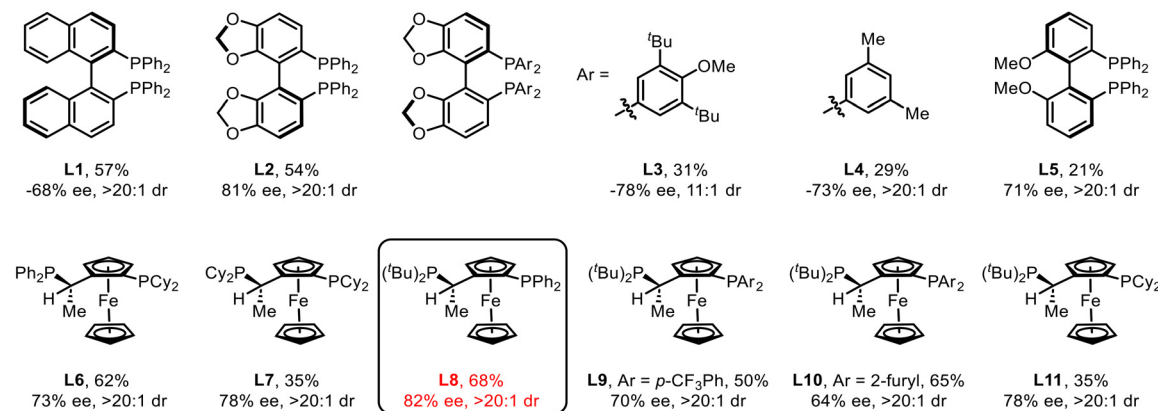
Optimization studies of the racemic process

To validate the feasibility of this strategy, we commenced our investigation on the racemic process with commercially available 3-hydroxyindole-2-carboxylate **1a** and enyne **2a** as model substrates. Employing Pd(OAc)₂ as the catalyst, Xantphos as the ligand, PhCOOH as the acid additive and DCM as the reaction medium, we successfully isolated product **3aa** in 30% yield with 10 : 1 dr (Table 1, entry 1). Subsequent optimization identified that Pd(acac)₂ or [Pd(π -allyl)Cl]₂ as the catalyst and toluene as the solvent significantly enhanced both productivity and diastereoselectivity (Table 1, entries 2–5).

Table 2 Optimization of the asymmetric reaction conditions^{a,b,c}



with [Pd(π -allyl)Cl]₂ as the catalyst, PhCOOH as an acid additive and toluene as the solvent



Entry	[Pd] source	Solvent	Additive	T/°C	Yield (%)	ee (%)	dr
1	[Pd(π -allyl)Cl] ₂	Toluene	PhCOOH	80	68	82	>20 : 1
2	[Pd(π -allyl)Cl] ₂	PhCF ₃	PhCOOH	80	75	86	>20 : 1
3	[Pd(π -allyl)Cl] ₂	Mesitylene	PhCOOH	80	76	82	>20 : 1
4	[Pd(π -allyl)Cl] ₂	THF	PhCOOH	80	65	67	15 : 1
5	Pd(dba) ₂	PhCF ₃	PhCOOH	80	71	86	>20 : 1
6	Pd(OAc) ₂	PhCF ₃	PhCOOH	80	63	81	>20 : 1
7	Pd(acac) ₂	PhCF ₃	PhCOOH	80	72	84	>20 : 1
8	[Pd(π -allyl)Cl] ₂	PhCF ₃	4-F-C ₆ H ₄ COOH	80	70	85	>20 : 1
9	[Pd(π -allyl)Cl] ₂	PhCF ₃	PhMe ₂ CCOOH	80	53	82	>20 : 1
10	[Pd(π -allyl)Cl] ₂	PhCF ₃	Ph ₃ CCOOH	80	67	84	>20 : 1
11	[Pd(π -allyl)Cl] ₂	PhCF ₃	1-AdCOOH	80	65	82	>20 : 1
12	[Pd(π -allyl)Cl] ₂	PhCF ₃	PhCOOH	60	71	90	>20 : 1
13	[Pd(π -allyl)Cl] ₂	PhCF ₃	PhCOOH	50	68	90	>20 : 1
14	[Pd(π -allyl)Cl] ₂	PhCF ₃	PhCOOH	40	63	92	>20 : 1
15	[Pd(π -allyl)Cl] ₂	PhCF ₃	PhCOOH	30	60	95	>20 : 1
16 ^d	[Pd(π -allyl)Cl] ₂	PhCF ₃	PhCOOH	30	86 (84) ^e	95	>20 : 1
17 ^d	[Pd(π -allyl)Cl] ₂	PhCF ₃	—	30	23	80	>20 : 1

^a Reaction conditions: **1a** (0.2 mmol), **2a** (0.4 mmol), [Pd] (10 mol%), ligand (20 mol%) and acid (20 mol%) in solvent (1.0 mL), under an argon atmosphere. ^b Yields of **3aa** were determined by GC with *n*-dodecane as the internal standard. ^c The dr and ee values were determined by chiral HPLC analysis. ^d 72 h. ^e Isolated yield.



Optimization studies of the asymmetric process

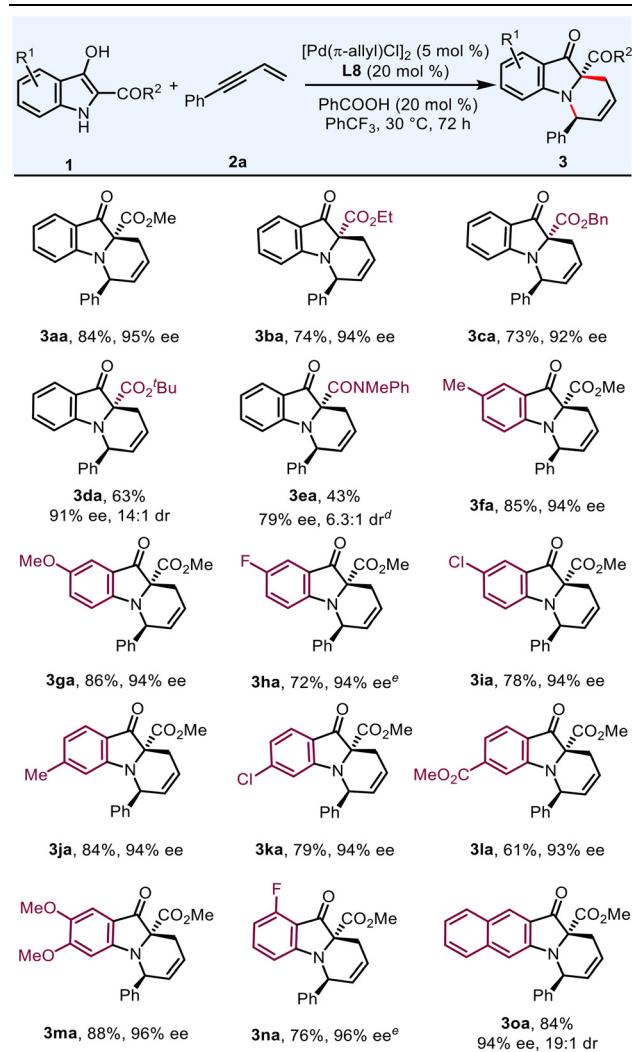
Encouraged by the success in racemic transformation, we endeavored to interpret this transformation into an enantioselective process. Combined with $[\text{Pd}(\pi\text{-allyl})\text{Cl}]_2$ as the catalyst, PhCOOH as the acid additive and toluene as the solvent, a variety of chiral BINAP-type bisphosphines were evaluated (Table 2, **L1–L4**). When (*S*)-SEGPHOS (**L2**) was employed as the chiral ligand, product **3aa** could be achieved in 54% yield with 81% ee and >20:1 dr. Modifying the electronic and steric properties of the ligands resulted in inferior outcomes (**L3** and **L4**). Upon assessing biphenyl-type and JosiPhos-type chiral ligands, **L8** emerged as the optimal, furnishing **3aa** in 68% yield with 82% ee. Solvent screening indicated that PhCF_3 provided the best results (Table 2, entries 1–4). Exploration of the palladium catalysts revealed that $[\text{Pd}(\pi\text{-allyl})\text{Cl}]_2$ was the most promising one (Table 2, entries 5–7). Different types of acids were then examined, but no superior yield and enantioselectivity were obtained (Table 2, entries 8–11). Next, lowering the reaction temperature can efficiently boost the ee values (Table 2, entries 12–15), and the enantioselectivity could be increased to 95% when the reaction was carried out at 30 °C (Table 2, entry 15). Elongation of the reaction time to 72 h afforded the product **3aa** in 84% isolated yield with 95% ee and >20:1 dr (Table 2, entry 16). Notably, in the absence of an acidic additive, the transformation still proceeded, albeit with reduced yield and enantioselectivity (Table 2, entry 17), underscoring the critical role of the acidic additive in this reaction. The absolute configuration of **3aa** was confirmed by X-ray diffraction and those of others were assigned by analogy.

Substrate scope in asymmetric transformation

Having determined the optimal conditions, we then investigated the substrate scope of 3-hydroxyindoles. As illustrated in Table 3, a preliminary examination of ester groups at the C2-position was initially performed. Switching the methyl group to other alkyl groups, such as ethyl and benzyl, this reaction could proceed smoothly as well and delivered **3ba** and **3ca** in 74% and 73% yields, respectively. A bulkier tertiary butyl group was also compatible with this catalytic system, yielding product **3da** in 63% yield with 91% ee and 14:1 dr. However, amide-substituted product **3ea** could only be isolated in 43% yield even under 60 °C for 5 days, with 50% starting material recovered. Both electron-donating (–Me and –OMe) and electron-withdrawing (–F, –Cl, and –CO₂Me) substituents at various positions of the aromatic rings were well tolerated, generating products **3fa–na** in 61–88% yields with 93–96% ee and >20:1 dr. In addition, polyaromatic fused rings, such as substrate **10a**, underwent this sequential hydroalkylation and hydroamination reaction smoothly, furnishing **30a** in 84% yield with 94% ee.

Subsequently, we directed our focus towards exploring the substrate scope of conjugated enynes (Table 4). The reaction involving enynes with electron-donating and electron-withdrawing substituents at the *para*-position of the phenyl ring generated chiral polycyclic indolines **3ab–ad** and **3af** in 72–88% yields with 93–96% ee. The introduction of a trifluoro-

Table 3 Substrate scope of 3-hydroxyindoles^{a,b,c}



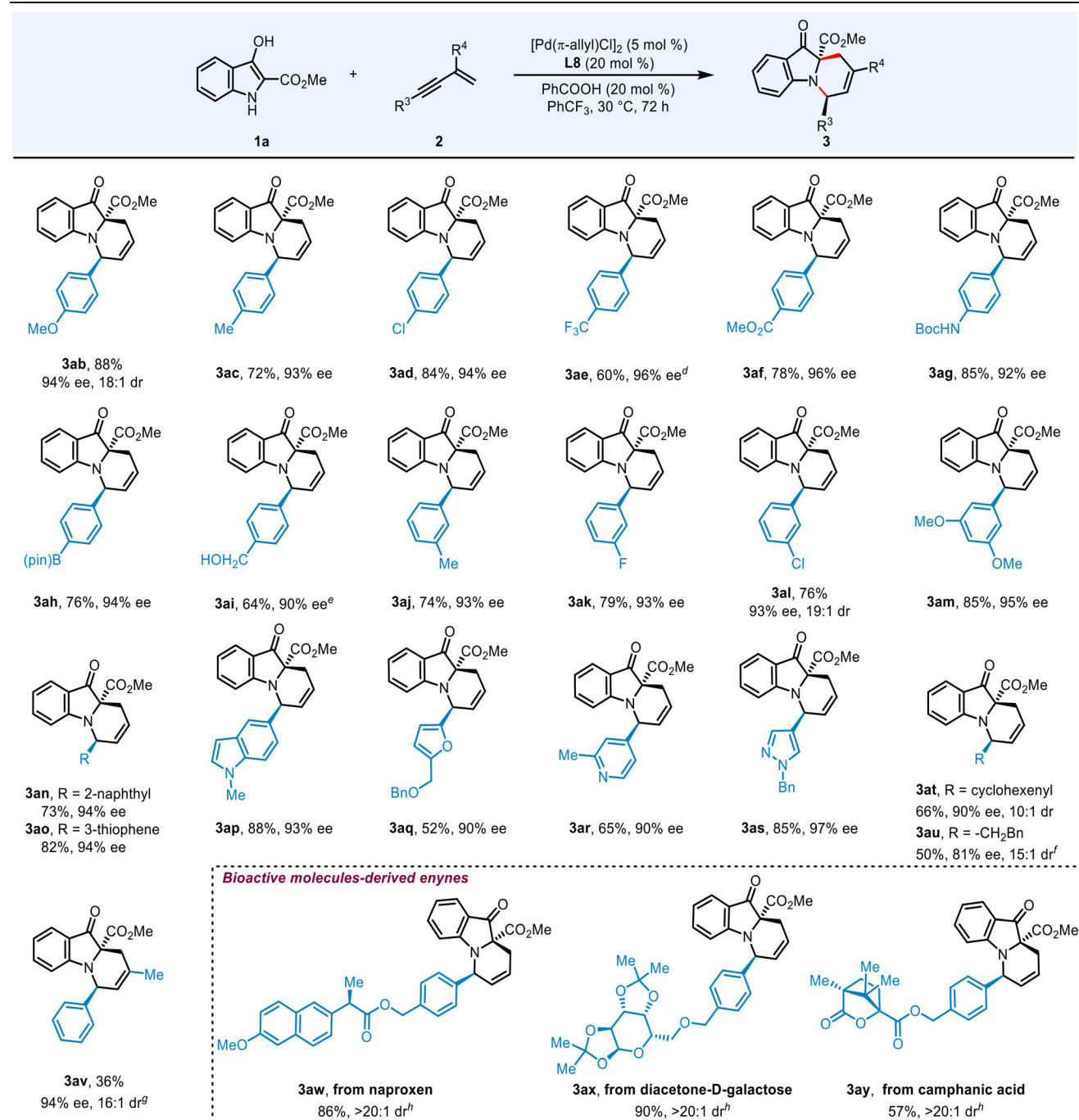
methyl group was also tolerated, delivering product **3ae** in 60% yield, albeit with the concomitant formation of a diene byproduct. Functional groups such as NHBoc (**3ag**), Bpin (**3ah**) and unprotected hydroxyl (**3ai**) were all well accommodated, maintaining good yields (64–85%) and stereoselectivities (90–94% ee, >20:1 dr). Excellent outcomes were also observed when *meta*-methyl, fluoride, chlorine and 3,5-dimethoxy were incorporated on the phenyl ring. In addition to aryl moieties, other fused arenes and heterocycles, such as naphthalene (**2n**), thiophene (**2o**), indole (**2p**), furan (**2q**), pyridine (**2r**) and parazole (**2s**), were all compatible with this transformation, delivering the desired products **3an–as** in 52–88% yields with 90–97% ee. Switching the aromatic rings to a cyclohexene motif, this reaction performed smoothly as well and compound **3at** was isolated in 66% yield with 90% ee. Efforts to broaden the diver-



sity of enyne substrates, such as alkyl enynes and those with substituents at R⁴, proved unsuccessful under the standard conditions. Under slightly modified conditions (with **L9** as the chiral ligand), **3au** was obtained in 50% yield and 81% ee, while the diene byproduct was also formed. In addition, utiliz-

ing **L2** as the chiral ligand enabled the reaction of **2v** to generate **3av** with good stereoselectivity, although in a lower yield at the expense of concurrent diene byproduct formation. The practicality of this protocol was assessed in the late stage sequential hydrofunctionalization of enynes derived from

Table 4 Substrate scope of 1,3-enynes^{a,b,c}



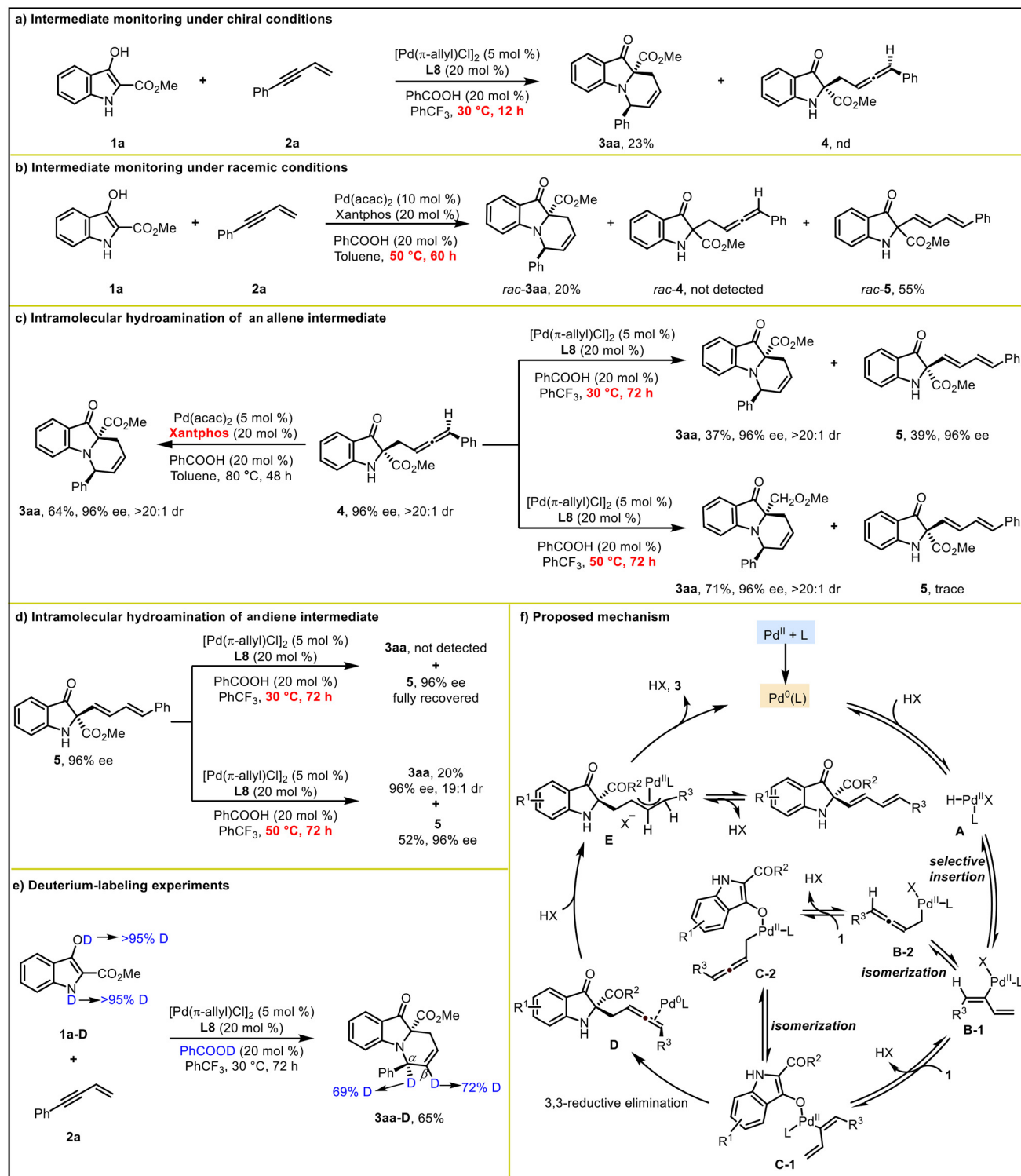
^a Reaction conditions: **1a** (0.2 mmol), **2** (0.4 mmol), [Pd(π-allyl)Cl]₂ (5 mol%), **L8** (20 mol%) and PhCOOH (20 mol%) in PhCF₃ (1.0 mL), 30 °C, 72 h, under an argon atmosphere. All products were obtained with >20:1 dr, unless otherwise stated. ^b Isolated yield. ^c The dr and ee values were determined by chiral HPLC analysis. ^d 40 °C. ^e 50 °C, 96 h. ^f **L9**, 50 °C, 72 h. ^g **L2** (20 mol%), 80 °C, 48 h. ^h The dr values were determined by ¹H NMR.



diverse biologically active molecules. Specifically, the reaction proceeded smoothly with enynes tethered to pharmaceuticals such as naproxen (**2w**), diacetone-D-galactose (**2x**), and camphanic acid (**2y**) to produce the target adducts in 57–90% yields with >20 : 1 dr.

Mechanistic studies

Based on previous reports,^{9,11} we hypothesized that the intermolecular hydroalkylation of 3-hydroxyindole **1** and enyne **2** should form an allene intermediate. Subsequent intra-

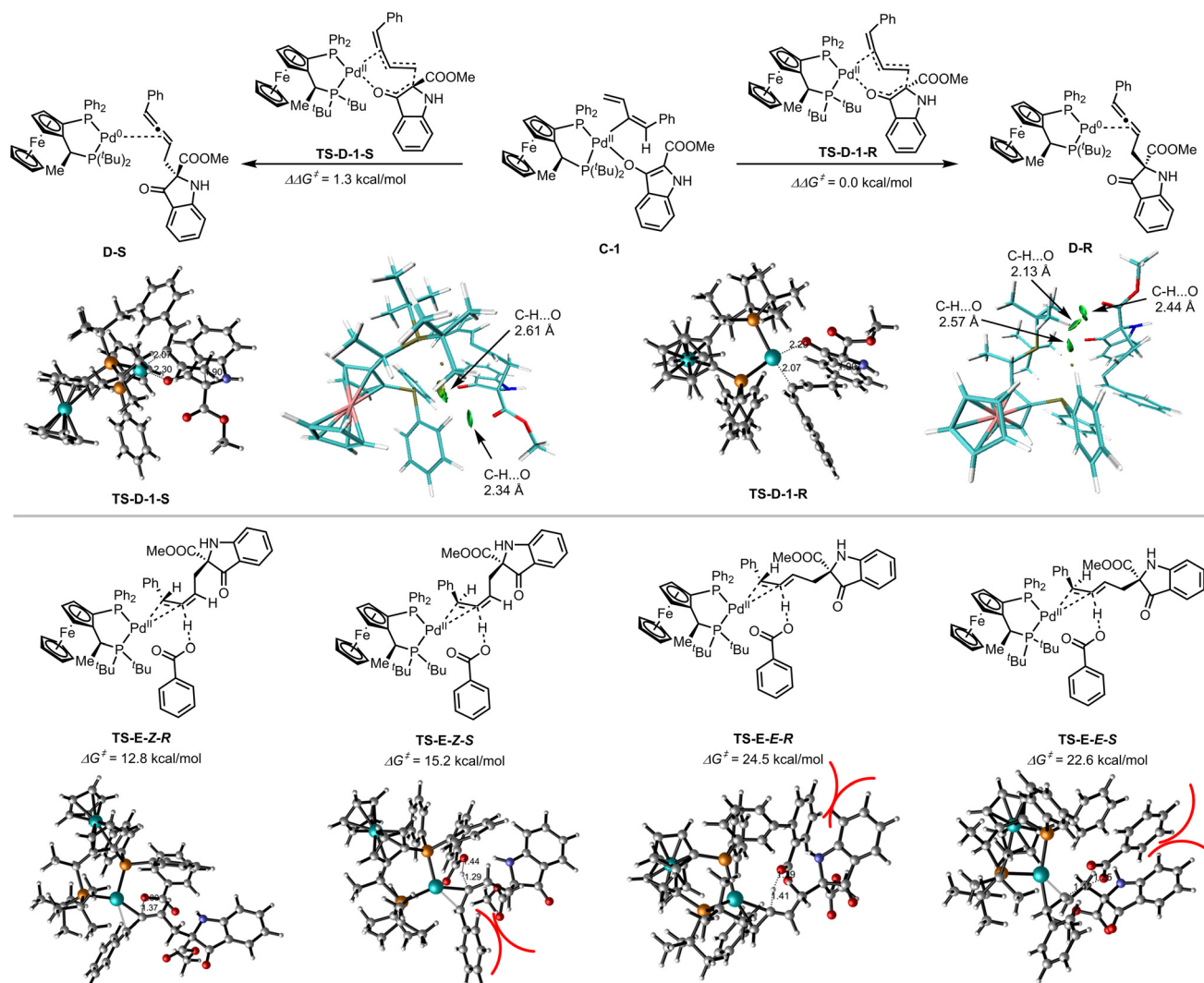


Scheme 2 Mechanistic studies.



molecular hydroamination of the allene was expected to produce the corresponding polycyclic indoline **3**. To verify this hypothesis, the reaction of **1a** with enyne **2a** was carried out under the standard conditions and quenched after 12 h. Then, the product **3aa** was isolated in 23% yield, with considerable amounts of **1a** remaining. However, the allene intermediate **4** was not detected (Scheme 2a). Furthermore, we attempted the synthesis of an allene intermediate in the presence of Pd(acac)₂ and Xantphos. When the reaction was performed at 50 °C, *rac*-**3aa** was formed in 20% yield, along with diene *rac*-**5** in 55% yield. Again, allene *rac*-**4** was not detected (Scheme 2b). To gain insight into the reaction process, we prepared enantio-enriched allene **4** *via* a palladium-catalyzed allylic reaction of allenyl carbonate (see the SI for more details).¹⁵ Treatment of allene **4** with Xantphos as the ligand afforded product **3aa** in 64% yield with 96% ee and >20:1 dr. Subsequently, allene **4** was subjected to asymmetric conditions with **L8** as the ligand, resulting in the intramolecular hydroamination product **3aa** in 37% yield, along with 39% yield of diene **5** in 96% ee.

Compound **3aa** was obtained in 71% yield with trace diene detected when the reaction was carried out at 50 °C (Scheme 2c). These data indicated that chiral allene **4** could efficiently transform into enantiopure **3aa** *via* axial-to-center chirality transfer. Moreover, the diene product might be generated *via* Pd–H migratory insertion of allene followed by β-H elimination.^{6m,16} These observations prompted us to speculate that diene might also serve as an intermediate in this Pd-catalyzed asymmetric sequential hydrofunctionalization reaction. To corroborate this hypothesis, chiral diene **5** was subjected to the conditions with **L8** as the ligand, but the diene was fully recovered (Scheme 2d, top panel). When the reaction was performed at 50 °C, product **3aa** was isolated in 20% yield with 96% ee (Scheme 2d, bottom panel). Collectively, these observations suggest that allene acts as the crucial intermediate of this sequential hydrofunctionalization, whereas diene was the by-product, as it cannot be converted into the target product under standard conditions. Furthermore, deuterium-labeling experiments were conducted. As shown in



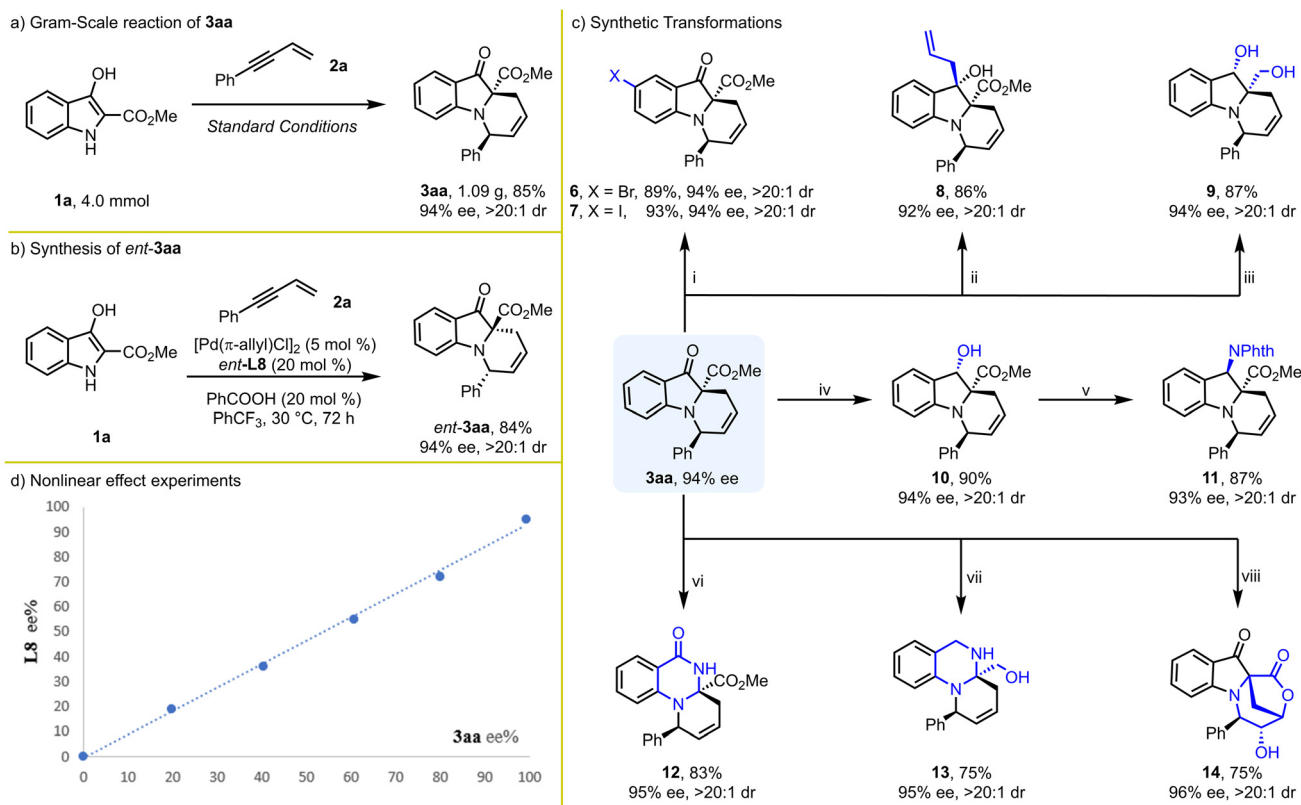
Scheme 3 Enantioselective model.



Scheme 2e, the reaction of 3-hydroxyindole **1a-D** with enyne **2a** in PhCF₃ in the presence of PhCOOD provided **3aa-D** in 65% yield, exhibiting 69% and 72% deuterium incorporation at the α - and β -positions, respectively. This result indicated that this reaction might involve two successive Pd-H migratory insertions.

Based on the above mechanistic studies and detailed density functional theory (DFT) calculations (see the SI for details), a plausible catalytic cycle for this reaction of conjugated enynes and 3-hydroxyindoles is proposed in Scheme 2f.^{9,11} Oxidative addition of Pd(0) with the acid affords PdH species **A**. Regioselective alkyne insertion to the PdH species **A** leads to the formation of η^1 -butadienyl-Pd intermediate **B-1**, which could be reversibly converted to the allenyl-Pd intermediate **B-2** *via* isomerization. Ligand exchange between 3-hydroxyindole **1** and intermediate **B-1** or **B-2** affords intermediates **C-1** or **C-2**, respectively. Due to the considerable energy barrier derived from computational studies, the pathway involving direct 1,1'-reductive elimination from intermediate **C-2** is energetically disfavored and can be effectively precluded. The chiral carbon center of the indole skeleton is mainly established *via* enantioselective 3,3-reductive elimination from intermediate **C-1** (Scheme 3). The reaction proceeds

preferentially through transition state **TS-D-1-R** *via* a 3,3-elimination pathway, which features an energy barrier of 1.3 kcal mol⁻¹ lower than that of the competing pathway *via* **TS-D-1-S**, thereby kinetically favoring the formation of the chiral allene intermediate **4** with *R*-configuration. To elucidate the origin of enantioselectivity, non-covalent interactions between the substrate and the chiral ligand moiety in transition states **TS-D-1-R** and **TS-D-1-S** were analyzed using the Independent Gradient Model based on Hirshfeld partition (IGMH).¹⁷ Structural analyses indicate that the more favorable transition state **TS-D-1-R** is stabilized by enhanced hydrogen-bonding interactions between C-H bonds of the chiral ligand and the oxygen atom of the indole framework. These interactions contribute significantly to the reduced activation energy barrier of **TS-D-1-R**, making it 1.3 kcal mol⁻¹ lower than that of **TS-D-1-S**. The direct electrophilic attack by the proton of benzoic acid on the palladium-activated allene intermediate **D** governs the enantioselectivity of the second stereocenter in the product. The pathway proceeding through the transition state **TS-E-Z-R** to form intermediate **E** exhibits an energy barrier of 12.8 kcal mol⁻¹, representing the kinetically most favorable route. Compared to the analogous pathway through the transition state **TS-E-Z-S**, the formation of intermediate **E** proceeds with



Scheme 4 Further study. Reagents and conditions: (i) for the synthesis of **6**: NBS (1.2 equiv.), THF/H₂O (9 : 1), rt, 6 h; for the synthesis of **7**: AuCl₃ (5 mol%), NIS (1.5 equiv.), DCE, rt, 12 h; (ii) allylMgBr (2.0 equiv.), THF, 0 °C–rt, 12 h; (iii) LiAlH₄ (LAH, 4.0 equiv.), THF, 40 °C, 6 h; (iv) NaBH₄, MeOH, 0.5 h; (v) Phthalimide (2.0 equiv.), PPh₃ (2.0 equiv.), DIAD (2.0 equiv.), THF, 0 °C–rt, 24 h; (vi) (1) NH₂OH·HCl (4.0 equiv.), pyridine (8.0 equiv.), EtOH, reflux, 24 h; (2) PPh₃ (20 mol%), CBr₄ (20 mol%), toluene, 80 °C, 24 h; (vii) (1) NH₂OH·HCl (4.0 equiv.), pyridine (8.0 equiv.), EtOH, reflux, 24 h; (2) DIBAL-H (5.0 equiv.), DCM, –78 °C–rt, 12 h; and (viii) K₂OsO₂(OH)₄ (20 mol%), NMO (4.2 equiv.), THF/H₂O, rt, 72 h.



the lowest energy barrier (12.8 kcal mol⁻¹ for **TS-E-Z-R** vs. 15.2 kcal mol⁻¹ for **TS-E-Z-S**). This distinct energy disparity substantiates the high enantioselectivity observed in the desired product **3aa**. The activation energies for forming the olefin architecture with an *E* geometry *via* transition states **TS-E-E-R** and **TS-E-E-S** are 24.5 and 22.6 kcal mol⁻¹, respectively. The disparity primarily stems from steric constraints imposed by the indole framework during the trajectory of electrophilic attack by benzoic acid. These values considerably exceed those required for the generation of the *Z*-olefin architecture. Given the computationally derived energy barriers, which are markedly elevated, this pathway can be confidently excluded.

Subsequently, the carboxylate anion in intermediate **E** can selectively abstract a hydrogen atom from either the indole nitrogen atom or the β-carbon atom of the ester group, leading to the formation of desired product **3aa** or the conjugated diene byproduct **5**, respectively. Overall, the formation of the conjugated diene byproduct proceeds reversibly *via* a lower energy barrier, enabling its generation under relatively mild reaction conditions and establishing it as the kinetically controlled product. In contrast, the pathway affording the desired product **3aa** involves a moderately higher activation barrier, suggesting its dominance under thermodynamic control. These computational insights align consistently with the experimental outcomes (Scheme 2c).

Further study

To exemplify the synthetic utility of the current protocol, a gram-scale reaction of **1a** and **2a** was performed, and product **3aa** was achieved in 85% yield with 94% ee and >20:1 dr (Scheme 4a). *Ent*-**3aa** was obtained in 84% yield and 94% ee by employing *ent*-**L8** as the chiral ligand (Scheme 4b). Several transformations with respect to **3aa** were then executed (Scheme 4c). Bromination and iodination of **3aa** were efficiently achieved using *N*-bromosuccinimide (NBS) and *N*-iodosuccinimide (NIS), producing compounds **6** and **7** with yields of 89% and 93%, respectively. The allyl Grignard reagent could selectively attack the ketone moiety to form tertiary alcohol **8** in 86% yield. In addition, the treatment of **3aa** with LiAlH₄ resulted in the isolation of diol **9** in 87% yield with excellent diastereoselectivity. Selective reduction of the carbonyl group in **3aa** to an alcohol **10** using NaBH₄ allowed for a subsequent Mitsunobu reaction to form the corresponding amide derivative **11**. Compounds **12** and **13** were easily constructed *via* the Beckmann rearrangement and DIBAL-H mediated ring-expansion rearrangement.¹⁸ In the presence of K₂OsO₂(OH)₄ and NMO, bridged compound **14** was formed *via* dihydroxylation and intramolecular esterification. The absolute configurations of **8** and **9** were confirmed by X-ray diffraction. Moreover, a linear relationship between the ee values of **L8** and the product **3aa** was observed, which indicated that one molecule of the chiral ligand participated in controlling the stereoselectivity of the reaction (Scheme 4d).

Conclusions

In summary, we have developed an unprecedented Pd-catalyzed sequential hydroalkylation and hydroamination of 1,3-enynes with 3-hydroxyindoles. This redox-neutral protocol offers an efficient approach for the synthesis of optically pure pyrido[1,2-*a*]indoles and derivatives bearing one tertiary stereocenter and one quaternary stereocenter. This reaction proceeds in a high atom- and step-economic manner with good functional group compatibility. Preliminary mechanistic investigations suggest that the transformation proceeds *via* an intermolecular enyne hydroalkylation pathway to form an allene intermediate. Subsequent intramolecular hydroamination of the allene intermediate occurs *via* an axial-to-center chirality transfer process. We believe this research will inspire and stimulate efforts for designing more innovative sequential hydrofunctionalization cyclization reactions, thereby providing a toolkit for the synthesis of chiral complex molecules, and driving the advancement of organic green chemistry. Computational studies were conducted to probe the origin of the enantioselectivities. Further investigations on other catalytic asymmetric sequential hydrofunctionalization reactions are currently underway in our laboratory.

Author contributions

Q. L., R. W. and T. W. contributed equally to this work.

Conflicts of interest

There are no conflicts to declare.

Data availability

The data supporting this article have been included as part of the supplementary information (SI). Supplementary information: detailed experimental procedures and characterization data for new compounds. See DOI: <https://doi.org/10.1039/d5gc05558j>.

CCDC 2268989 (**3aa**), 2321444 (**8**) and 2321211 (**9**) contain the supplementary crystallographic data for this paper.^{19a-c}

Acknowledgements

The authors acknowledge generous financial support from the National Natural Science Foundation of China (22371299), the Natural Science Foundation of Jiangsu Province (BK20242068 and BK20251564), the Open Project of State Key Laboratory of Natural Medicines (SKLNMKF202401), the China Postdoctoral Science Foundation (2024M763657), the Postdoctoral Fellowship Program of CPSF (GZB20250246), the Project Program of the State Key Laboratory of Natural Medicines (SKLNMZZ202211), the Fundamental Research Funds for the



Central Universities (2632024ZD09 and 2632025PY03), the Jiangsu Funding Program for Excellent Postdoctoral Talent (2025ZB316), and the Innovation and Entrepreneurship (Shuangchuang) Program of Jiangsu Province (2024). We are also grateful to the High-Performance Computing Center of Nanjing University for performing the numerical calculations in this paper on its blade cluster system.

References

- (a) J. H. Clark, *Green Chem.*, 2006, **8**, 17; (b) I. T. Horváth and P. T. Anastas, *Chem. Rev.*, 2007, **107**, 2169; (c) R. Noyori, *Nat. Chem.*, 2009, **1**, 5; (d) P. Anastas and N. Eghbali, *Chem. Soc. Rev.*, 2010, **39**, 301; (e) P. J. Dunn, *Chem. Soc. Rev.*, 2012, **41**, 1452.
- For selected reviews, see: (a) L. Huang, M. Arndt, K. Gooßen, H. Heydt and L. J. Gooßen, *Chem. Rev.*, 2015, **115**, 2596; (b) P. Koschker and B. Breit, *Acc. Chem. Res.*, 2016, **49**, 1524; (c) J. Chen, J. Guo and Z. Lu, *Chin. J. Chem.*, 2018, **36**, 1075; (d) G. Li, X. Huo, X. Jiang and W. Zhang, *Chem. Soc. Rev.*, 2020, **49**, 2060; (e) J. Li and Y. Shi, *Chem. Soc. Rev.*, 2022, **51**, 6757; (f) Y. Li, X. Lu and Y. Fu, *CCS Chem.*, 2024, **6**, 1130.
- For selected reviews, see: (a) J. Chen and Z. Lu, *Org. Chem. Front.*, 2018, **5**, 260; (b) Y. He, J. Chen, X. Jiang and S. Zhu, *Chin. J. Chem.*, 2022, **40**, 651; (c) X.-Y. Sun, B.-Y. Yao, B. Xuan, L.-J. Xiao and Q.-L. Zhou, *Chem. Catal.*, 2022, **2**, 3140; (d) W. Zhao, H.-X. Lu, W.-W. Zhang and B.-J. Li, *Acc. Chem. Res.*, 2023, **56**, 308. For selected examples, see: (e) A. L. Rez-nichenko, H. N. Nguyen and K. C. Hultsch, *Angew. Chem., Int. Ed.*, 2010, **49**, 8984; (f) K. Manna, S. Xu and A. D. Sadow, *Angew. Chem., Int. Ed.*, 2011, **50**, 1865; (g) H.-L. Teng, Y. Luo, B. Wang, L. Zhang, M. Nishiura and Z. Hou, *Angew. Chem., Int. Ed.*, 2016, **55**, 15406; (h) Y. Xi and J. F. Hartwig, *J. Am. Chem. Soc.*, 2016, **138**, 6703; (i) Y. Xi, S. Ma and J. F. Hartwig, *Nature*, 2020, **588**, 254; (j) F. Zhou, Y. Zhang, X. Xu and S. Zhu, *Angew. Chem., Int. Ed.*, 2019, **58**, 1754; (k) Y. He, C. Liu, L. Yu and S. Zhu, *Angew. Chem., Int. Ed.*, 2020, **59**, 9186; (l) X. Ren, Z. Wang, C. Shen, X. Tian, L. Tang, X. Ji and K. Dong, *Angew. Chem., Int. Ed.*, 2021, **60**, 17693; (m) T. Qin, G. Lv, H. Miao, M. Guan, C. Xu, G. Zhang, T. Xiong and Q. Zhang, *Angew. Chem., Int. Ed.*, 2022, **61**, e202201967; (n) H. S. Slocumb, S. Nie, V. M. Dong and X.-H. Yang, *J. Am. Chem. Soc.*, 2022, **144**, 18246; (o) W. Zhao, K.-Z. Chen, A.-Z. Li and B.-J. Li, *J. Am. Chem. Soc.*, 2022, **144**, 13071.
- For selected reviews, see: (a) A. M. Haydl, B. Breit, T. Liang and M. J. Krische, *Angew. Chem., Int. Ed.*, 2017, **56**, 11312; (b) J. Chen, W.-T. Wei, Z. Li and Z. Lu, *Chem. Soc. Rev.*, 2024, **53**, 7566. For selected examples, see: (c) Q.-A. Chen, Z. Chen and V. M. Dong, *J. Am. Chem. Soc.*, 2015, **137**, 8392; (d) P. Koschker, M. Kähny and B. Breit, *J. Am. Chem. Soc.*, 2015, **137**, 3131; (e) F. A. Cruz and V. M. Dong, *J. Am. Chem. Soc.*, 2017, **139**, 1029; (f) F.-T. Sheng, S.-C. Wang, J. Zhou, C. Chen, Y. Wang and S. Zhu, *ACS Catal.*, 2023, **13**, 3841; (g) A. Huang, H.-R. Xu, Z.-J. Yang, X.-S. Xue and Z.-T. He, *Nat. Synth.*, 2025, **4**, 1565.
- For selected reviews, see: (a) R. Blicek, M. Taillefer and F. Monnier, *Chem. Rev.*, 2020, **120**, 13545; (b) S. V. Sieger, I. Lubins and B. Breit, *ACS Catal.*, 2022, **12**, 11301. For selected examples, see: (c) K. L. Butler, M. Tragni and R. A. Widenhoefer, *Angew. Chem., Int. Ed.*, 2012, **51**, 5175; (d) M. L. Cooke, K. Xu and B. Breit, *Angew. Chem., Int. Ed.*, 2012, **51**, 10876; (e) K. Xu, N. Thieme and B. Breit, *Angew. Chem., Int. Ed.*, 2014, **53**, 2162; (f) C. Li, M. Kähny and B. Breit, *Angew. Chem., Int. Ed.*, 2014, **53**, 13780; (g) A. M. Haydl, K. Xu and B. Breit, *Angew. Chem., Int. Ed.*, 2015, **54**, 7149; (h) Z. Yang and J. Wang, *Angew. Chem., Int. Ed.*, 2021, **60**, 27288; (i) M.-Q. Tang, Z.-J. Yang, A.-J. Han and Z.-T. He, *Angew. Chem., Int. Ed.*, 2025, **64**, e202413428.
- For selected reviews, see: (a) G. J. P. Perry, T. Jia and D. J. Procter, *ACS Catal.*, 2020, **10**, 1485; (b) N. J. Adamson and S. J. Malcolmson, *ACS Catal.*, 2020, **10**, 1060; (c) A. Flaget, C. Zhang and C. Mazet, *ACS Catal.*, 2022, **12**, 15638; (d) Y. C. Wang, J.-B. Liu and Z.-T. He, *Chin. J. Org. Chem.*, 2023, **43**, 2614. For selected examples, see: (e) S.-Z. Nie, R. T. Davison and V. M. Dong, *J. Am. Chem. Soc.*, 2018, **140**, 16450; (f) N. J. Adamson, K. C. E. Wilbur and S. J. Malcolmson, *J. Am. Chem. Soc.*, 2018, **140**, 2761; (g) Q. Zhang, H. Yu, L. Shen, T. Tang, D. Dong, W. Chai and W. Zi, *J. Am. Chem. Soc.*, 2019, **141**, 14554; (h) Q. Zhang, D. Dong and W. Zi, *J. Am. Chem. Soc.*, 2020, **142**, 15860; (i) A. Y. Jiu, H. S. Slocumb, C. S. Yeung, X.-H. Yang and V. M. Dong, *Angew. Chem., Int. Ed.*, 2021, **60**, 19660; (j) Q. Li, Z. Wang, V. M. Dong and X.-H. Yang, *J. Am. Chem. Soc.*, 2023, **145**, 3909; (k) X.-X. Chen, H. Luo, Y.-W. Chen, Y. Liu and Z.-T. He, *Angew. Chem., Int. Ed.*, 2023, **62**, e202307628; (l) S.-Q. Yang, A.-J. Han, Y. Liu, X.-Y. Tang, G.-Q. Lin and Z.-T. He, *J. Am. Chem. Soc.*, 2023, **145**, 3915; (m) M.-Q. Tang, Z.-J. Yang and Z.-T. He, *Nat. Commun.*, 2023, **14**, 6303; (n) Y.-C. Wang, Z.-X. Xiao, M. Wang, S.-Q. Yang, J.-B. Liu and Z.-T. He, *Angew. Chem., Int. Ed.*, 2023, **62**, e202215568.
- For review, see: (a) L. Li, S. Wang, A. Jakhar and Z. Shao, *Green Synth. Catal.*, 2023, **4**, 124. For examples, see: (b) Y. Yang, I. B. Perry, G. Lu, P. Liu and S. L. Buchwald, *Science*, 2016, **353**, 144; (c) Y. Huang, J. del Pozo, S. Torker and A. H. Hoveyda, *J. Am. Chem. Soc.*, 2018, **140**, 2643; (d) L. Bayeh-Romero and S. L. Buchwald, *J. Am. Chem. Soc.*, 2019, **141**, 13788; (e) D.-W. Gao, Y. Xiao, M. Liu, Z. Liu, M. K. Karunananda, J. S. Chen and K. M. Engle, *ACS Catal.*, 2018, **8**, 3650; (f) H. Tsukamoto, T. Konno, K. Ito and T. Doi, *Org. Lett.*, 2019, **21**, 6811; (g) N. J. Adamson, H. Jeddi and S. J. Malcolmson, *J. Am. Chem. Soc.*, 2019, **141**, 8574; (h) S.-Q. Yang, Y.-F. Wang, W.-C. Zhao, G.-Q. Lin and Z.-T. He, *J. Am. Chem. Soc.*, 2021, **143**, 7285; (i) C. You, M. Shi, X. Mi and S. Luo, *Nat. Commun.*, 2023, **14**, 2911.
- For selected reviews, see: (a) X. Zeng, *Chem. Rev.*, 2013, **113**, 6864; (b) Z. Cheng, J. Guo and Z. Lu, *Chem. Commun.*, 2020, **56**, 2229. For selected examples, see: (c) A. Heutling, F. Pohlki, I. Bytschkov and S. Doye, *Angew. Chem., Int. Ed.*,



- 2005, **44**, 2951; (d) Y. Lee, H. Jang and A. H. Hoveyda, *J. Am. Chem. Soc.*, 2009, **131**, 18234; (e) S.-L. Shi and S. L. Buchwald, *Nat. Chem.*, 2015, **7**, 38; (f) Z. Zuo, J. Yang and Z. Huang, *Angew. Chem., Int. Ed.*, 2016, **55**, 10839; (g) J. Guo, X. Shen and Z. Lu, *Angew. Chem., Int. Ed.*, 2017, **56**, 615; (h) J. Guo, B. Cheng, X. Shen and Z. Lu, *J. Am. Chem. Soc.*, 2017, **139**, 15316; (i) J. Guo, H. Wang, S. Xing, X. Hong and Z. Lu, *Chem*, 2019, **5**, 881; (j) M. Hu and S. Ge, *Nat. Commun.*, 2020, **11**, 765; (k) D.-W. Gao, Y. Gao, H. Shao, T.-Z. Qiao, X. Wang, B. B. Sanchez, J. S. Chen, P. Liu and K. M. Engle, *Nat. Catal.*, 2020, **3**, 23; (l) J. Chen, X. Shen and Z. Lu, *J. Am. Chem. Soc.*, 2020, **142**, 14455; (m) S. Jin, K. Liu, S. Wang and Q. Song, *J. Am. Chem. Soc.*, 2021, **143**, 13124; (n) S. Jin, J. Li, K. Liu, W.-Y. Ding, S. Wang, X. Huang, X. Li, P. Yu and Q. Song, *Nat. Commun.*, 2022, **13**, 3524; (o) S. Wang, K. Chen, J. Niu, X. Guo, X. Yuan, J. Yin, B. Zhu, D. Shi, W. Guan, T. Xiong and Q. Zhang, *Angew. Chem., Int. Ed.*, 2024, **63**, e202410833; (p) H. Wang, X. Jie, Q. Chong and F. Meng, *Nat. Commun.*, 2024, **15**, 3427.
- 9 L. Li, S. Wang, P. Luo, R. Wang, Z. Wang, X. Li, Y. Deng, F. Peng and Z. Shao, *Nat. Commun.*, 2021, **12**, 5667.
- 10 W. Lu, Y. Zhao and F. Meng, *J. Am. Chem. Soc.*, 2022, **144**, 5233.
- 11 Q. Li, X. Fang, R. Pan, H. Yao and A. Lin, *J. Am. Chem. Soc.*, 2022, **144**, 11364.
- 12 B.-Y. Xie and Z.-T. He, *ACS Catal.*, 2024, **14**, 9742.
- 13 (a) D. Zhang, M. Li, J. Li, A. Lin and H. Yao, *Nat. Commun.*, 2021, **12**, 6627; (b) Q. Li, J. Li, J. Zhang, S. Wu, Y. Zhang, A. Lin and H. Yao, *Angew. Chem., Int. Ed.*, 2023, **62**, e202313404; (c) Q. Wu, Q. Zhang, S. Yin, A. Lin, S. Gao and H. Yao, *Angew. Chem., Int. Ed.*, 2023, **62**, e202305518; (d) M. Xu, Q. Lu, B. Gong, W. Ti, A. Lin, H. Yao and S. Gao, *Angew. Chem., Int. Ed.*, 2023, **62**, e202311540.
- 14 (a) G. Bartoli, G. Bencivenni and R. Dalpozzo, *Chem. Soc. Rev.*, 2010, **39**, 4449; (b) B. P. Pritchett and B. M. Stoltz, *Nat. Prod. Rep.*, 2018, **35**, 559; (c) A. E. Nugroho, W. Zhang, Y. Hirasawa, Y. Tang, C. P. Wong, K. Kaneda, A. H. A. Hadi and H. Morita, *J. Nat. Prod.*, 2018, **81**, 2600; (d) Y. Hong, Y. Y. Zhu, Q. He and S.-X. Gu, *Bioorg. Med. Chem.*, 2022, **55**, 116597.
- 15 S. Song and S. Ma, *Chin. J. Chem.*, 2020, **38**, 1233.
- 16 (a) I. Crouch, T. Dreier and D. Frantz, *Angew. Chem., Int. Ed.*, 2011, **50**, 6128; (b) G. Cera, M. Lanzi, F. Bigi, R. Maggi, M. Malacriab and G. Maestri, *Chem. Commun.*, 2018, **54**, 14021.
- 17 T. Lu and Q. Chen, *J. Comput. Chem.*, 2022, **43**, 539.
- 18 (a) H. Zhao, C. P. Vandenbossche, S. G. Koenig, S. P. Singh and R. P. Bakale, *Org. Lett.*, 2008, **10**, 505; (b) Y. Iwama, K. Okano, K. Sugimoto and H. Tokuyama, *Org. Lett.*, 2012, **14**, 2320; (c) S.-L. Cai, Y. Li, C. Yang, J. Sheng and X.-S. Wang, *ACS Catal.*, 2019, **9**, 10299.
- 19 (a) CCDC 2268989: Experimental Crystal Structure Determination, 2026, DOI: [10.5517/ccdc.csd.cc2g526y](https://doi.org/10.5517/ccdc.csd.cc2g526y); (b) CCDC 2321444: Experimental Crystal Structure Determination, 2026, DOI: [10.5517/ccdc.csd.cc2hxn9d](https://doi.org/10.5517/ccdc.csd.cc2hxn9d); (c) CCDC 2321211: Experimental Crystal Structure Determination, 2026, DOI: [10.5517/ccdc.csd.cc2hxdsm](https://doi.org/10.5517/ccdc.csd.cc2hxdsm).

